The Noise Temperature of an Arbitrarily Shaped Microwave Cavity with Application to a Set of Millimetre Wave Primary Standards

W. C. Daywitt

Abstract. An expression for the noise temperature of an arbitrarily shaped microwave cavity is derived and illustrated. The result is applied to a horn/cavity noise source and forms the basis for a set of primary reference noise standards that covers the millimetre wave frequency range in thirteen bands from WR-42 to WR-3. Power attenuation coefficients for sectoral horns are also presented.

1. Introduction

A microwave cavity is defined here as a cavity with one output line that supports a single propagating mode. The line can be a coaxial or a hollow waveguide transmission line or, as in the case of the millimetre wave noise standards to be discussed, a pyramidal horn. Thermal radiation from the cavity walls is conducted by the line to an output connector where it appears as an available, broadband (spectral) noise power.

The line itself emits and absorbs radiation due to its own dissipative losses, changing the magnitude of the noise available at the output connector. This change is called excess noise and is a positive or negative addition to the cavity wall noise depending upon whether the physical temperature of the line is greater or less, respectively, than the physical temperature of the cavity. An accurate estimation of this excess noise is central to the design of primary noise standards but, unfortunately, accurate estimates are increasingly difficult to achieve in the higher millimetre wave frequency bands as line losses increase with frequency.

It was the larger noise temperature errors caused by the higher line losses that led to the following horn/cavity design and the requisite theory. And, while the horn/cavity configuration is not new, the rigorous mathematical foundation required of a primary reference standard is. The most accurate description available to date [1] relies on the plane wave scattering matrix theory of antennas that is valid only in the far and radiative near fields, but excludes the reactive near field which is unavoidable in noise standard design. The present work corrects this shortcoming, adds a few new insights to the theory of thermal sources, and presents equations for the attenuation coefficients of sectoral horns that are unavailable in the open literature.

W. C. Daywitt: Reference Grade Standards, 140 Iroquois Dr., Boulder, CO 80303, USA.

2. Noise Temperature of an Arbitrarily Shaped Microwave Cavity

The spectral power of a noise source is the power per unit bandwidth available at the source's output port. This is true whatever the character of the source, whether solid state, gas discharge or thermal in nature. This power is conveniently described in terms of a noise temperature which is defined [2] as the spectral power divided by Boltzmann's constant, making the noise temperature of a thermal source of uniform physical or thermodynamic temperature equal to its thermodynamic temperature (quantum effects are discussed in Appendix A).

The purpose of this section is to derive a fundamental relationship for the noise temperature that is independent of the physical geometry of the cavity and the emissivity of the cavity walls. The result provides the foundation needed in Section 4 to describe the output of a horn/cavity type of source.

A cavity of arbitrary shape is shown in Figure 1 where T_n is the output noise temperature and T is the cavity wall temperature which varies with position. The wall temperature is constant (T_m) in the

metrologia

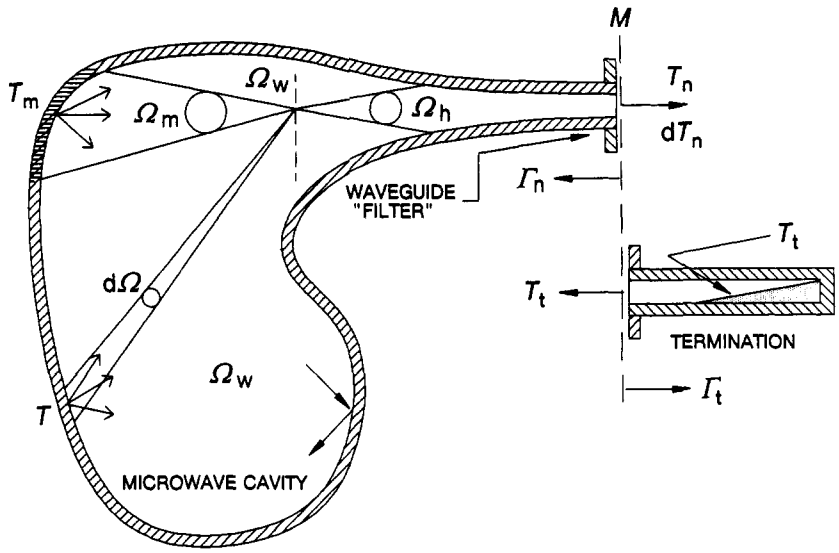

Figure 1. Microwave cavity and termination.

solid angle Ω_m shown in the figure. A coordinate system is erected within the cavity to specify the condition and temperature of the walls at any point, the elemental areas of which are included in the differential solid angles $d\Omega$. To understand the following development, it is important to realize that the solid angles are only a book-keeping device that catalogue the location of the radiant sources within the wall. They are not the solid angles used in antenna theory to sum the total radiation entering an antenna aperture from a particular direction.

The differential area subtended by $d\Omega$ emits a radiant energy that is proportional to the thermodynamic temperature T. A portion of this energy proceeds directly via the waveguide to the output flange. The remaining portion reflects off the interior walls numerous times, being slightly reduced in intensity at each reflection by the wall losses. The entire contribution from $d\Omega$ to the output noise power can be expressed generally as

$$M\,dT_n = TS\,d\Omega, \tag{1}$$

where S contains the effects of both the direct and indirect components of the energy. The function S does not contain the temperature explicitly, although it does so implicitly due to the fact that the emissivity and absorptivity of the wall depend upon the electrical resistivity whose magnitude is influenced by the temperature. The output mismatch factor M [4] in (1), which is not unique to the area in $d\Omega$, is required because the right side of (1) refers to the net or delivered power leaving the output flange while the noise temperature corresponds to the available power.

It should be clear that S is a complicated function which contains sums and integrals over the reflection components of the energy generated in $d\Omega$. Equation (29) of reference [1] is an example of the type of series encountered in a simple case where the calculations can be approximated by a diffraction model [3].

Since the radiation from different points on the cavity wall is uncorrelated, the total noise temperature T_n is given by the linear sum of the differential contributions

$$MT_n = \int TS\,d\Omega, \tag{2}$$

where the integral includes the entire internal surface area of the cavity.

Suppose that the termination (whose physical temperature is T_t) shown in Figure 1 is now attached to the cavity. Suppose also that the cavity has the same uniform temperature T_t. Then, the noise temperature of the termination is T_t. But, the noise temperature T_n of the cavity must also be T_t or there will be an imbalance in energy transfer between cavity and termination and one or the other will heat up. That this imbalance is never seen in practice is manifest in the second law of thermodynamics [5]. In other words, the second law and (2) imply that

$$\int T_t S_t\,d\Omega = M_t T_t, \tag{3}$$

where the subscripts on S and M are used temporarily to emphasize that all wall resistivities are to be evaluated at the temperature T_t. Since the T_t on the left side of (3) is constant, it can be removed from under the integral sign and cancelled with the T_t on the right side, leaving

$$\int S_t\,d\Omega = M_t. \tag{4}$$

This result was easily derived by the preceding thermodynamic arguments. Deriving it from electromagnetic theory alone, however, is practically impossible except under very special circumstances. One of these special circumstances is presented in the next section where the case of cascaded 2-ports is examined.

The special case in the next section suggests that the relationship in (4) is more general than thermodynamics alone would imply. In particular, thermodynamics says that (4) is true when the cavity wall is at some uniform temperature T_t. But this is only an apparent restriction that arises from the state of thermodynamic equilibrium requiring that the cavity wall emissions and absorptions be equal. The important point here is that (4) is true in general no matter what the temperature distribution of the cavity wall. In other words, (4) can be replaced by

$$\int S\,\mathrm{d}\Omega = M. \tag{5}$$

Equation (5) is true in general and says that the source's mismatch factor M is equal to the integral over the cavity surface. It is interesting to note in passing that the surface integral vanishes for the pathological case of a lossless cavity since the mismatch factor vanishes for the lossless case.

Suppose now that a part of the cavity is maintained at a uniform temperature T_m. Then, the integral in (5) can formally be split into two pieces, one over Ω_m and one over the remaining part of the cavity $\Omega_w + \Omega_h$. This procedure leads to

$$\int_m S\,\mathrm{d}\Omega = M - \int_{w+h} S\,\mathrm{d}\Omega. \tag{6}$$

Dividing the remaining cavity into Ω_w and Ω_h was done to serve a later purpose but does not affect the present development.

Inserting (6) into (2) yields

$$MT_n = MT_m + \int_{w+h} (T - T_m)\, S\,\mathrm{d}\Omega, \tag{7}$$

and dividing by M gives the sought-after noise temperature

$$T_n = T_m + \int_{w+h} (T - T_m)\, S'\,\mathrm{d}\Omega, \tag{7'}$$

where $S' \equiv S/M$ is independent of the termination reflection coefficient Γ_t in Figures 1 and 2. The second term in these two equations is the excess noise which describes an excess above or below what is present if the cavity were at a uniform temperature $T = T_m$.

Although (7') is generally valid, its usefulness depends upon a number of things. For example, if the wall subtended by Ω_m is highly reflective, then both terms on the right side are large and the resulting S' is a significant part of the whole and must be accurately evaluated where $T - T_m$ is not small. However, $T - T_m$ cannot be small everywhere if T_m is different from ambient temperature because the output flange of the cavity must be maintained at room temperature. Therefore, to design an accurate standard, the cavity geometry must be arranged so that S' is small and accurately calculable where $T - T_m$ is significant. One design that fulfills these requirements is presented in Section 4.

3. Cascaded 2-Ports

This section illustrates the identity in (5) for a situation, cascaded microwave 2-ports, where the integrals can easily be determined. Figure 2 shows a diagram of two 2-ports in cascade terminated by a load. The thermodynamic temperatures of the termination and the 2-ports are T_m, T_1, and T_2. The mismatch factors at the three reference planes are M_1, M_2 and M, and η_1, η_2 and η are 2-port efficiencies which are defined as net output to net input powers [4].

The noise power leaving the 2-ports and termination is [4]

$$\begin{aligned} MT_n = {} & M_1 T_m \eta + T_1 (M_2 - M_1 \eta_1)\eta_2 \\ & + T_2 (M - M_2 \eta_2), \end{aligned} \tag{8}$$

while applying (2) to the configuration in Figure 2 leads to

$$MT_n = T_m \int_m S\,\mathrm{d}\Omega + T_1 \int_1 S\,\mathrm{d}\Omega + T_2 \int_2 S\,\mathrm{d}\Omega. \tag{9}$$

Equating coefficients between (8) and (9) yields

$$\begin{aligned} \int_m S\,\mathrm{d}\Omega &= M_1 \eta = M_1 \eta_1 \eta_2 \\ \int_1 S\,\mathrm{d}\Omega &= (M_2 - M_1 \eta_1)\eta_2 \\ \int_2 S\,\mathrm{d}\Omega &= M - M_2 \eta_2 \end{aligned} \tag{10}$$

for the surface integrals.

Summing the right and left sides of the three expressions in (10) leads to

$$\int_m S\,\mathrm{d}\Omega + \int_1 S\,\mathrm{d}\Omega + \int_2 S\,\mathrm{d}\Omega = \int S\,\mathrm{d}\Omega = M \tag{11}$$

in agreement with (5).

The relation $\eta = \eta_1 \eta_2$ used in the first expression in (10) comes from microwave circuit theory [6]. Thermodynamics obtains it as the special case (4): again, summing the expressions in (10) (but using the first equality in the first expression this time) and inserting into (4) yields

$$M_1 \eta + (M_2 - M_1 \eta_1)\eta_2 + M - M_2 \eta_2 = M, \tag{12}$$

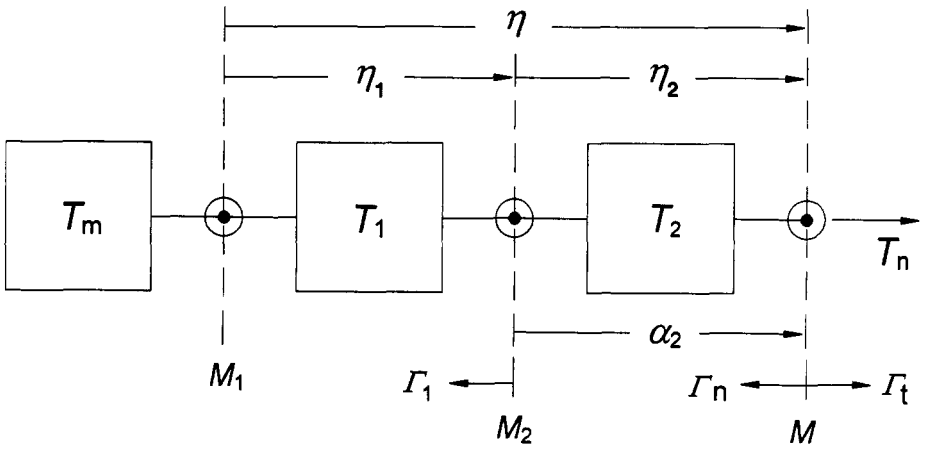

Figure 2. Cascaded 2-ports.

or

$$\eta_t = \eta_{1t}\eta_{2t} \tag{13}$$

for the thermodynamic result (the subscripts again indicate that the resistivities are evaluated at the temperature T_t). This is clearly consistent with the microwave theory result $\eta = \eta_1 \eta_2$.

A closer look at the second 2-port in Figure 2 will be useful in the next section. A second efficiency, α_2, is defined for this 2-port and is called the *noise efficiency* to distinguish it from the η efficiencies. It is the ratio of available output to input powers through the 2-port. Using microwave circuit theory [4],

$$\alpha_2 = \frac{(1-|\Gamma_1|^2)|S_{21}|^2}{(1-|\Gamma_m|^2)|1-S_{11}\Gamma_1|^2}, \tag{14}$$

where the S_{ij} are scattering coefficients for the second 2-port and Γ_1 and Γ_n are reflection coefficients.

The expression in (14) holds for any 2-port. If the 2-port is a piece of uniform transmission line or a smooth line that is gradually expanding or contracting, then $S_{11} = S_{22} = 0$ and the noise efficiency becomes

$$\alpha_2 = \frac{(1-|\Gamma_1|^2)|S_{21}|^2}{1-|S_{21}\Gamma_1|^2}. \tag{15}$$

If $\Gamma_1 = 0$ also, then

$$\alpha_2 = |S_{21}|^2 = 10^{-A/10}, \tag{16}$$

where A is the decibel attenuation through the second 2-port and accounts for the dissipative line loss. This attenuation can be calculated accurately. A process similar to the two steps leading from (14) to (16) is repeated in the next section where the horn assumes a position analogous to the second 2-port.

4. Noise Temperature for a Horn/Cavity Design

A set of millimetre wave, primary noise standards has been designed [7] using a horn/cavity configuration, a simplified machine drawing of which is shown in Figure 3. The configuration consists of a load that is partly immersed in liquid nitrogen (the cavity shown in the figure is on its side: when in use it is set upright with the horn at the top), a circular cylinder that holds the load, the horn, and a flexible radiation shield that keeps ambient radiation out of the cavity while allowing the horn to be attached to a system without supporting the weight of the entire standard.

The region of the cavity surrounding and just to the right of the load is maintained at the boil-off temperature of the nitrogen liquid. Further to the right, the cylinder wall rises in temperature until it attains ambient or room temperature at the radiation shield. That part of the copper horn to the right of the shield is maintained at ambient temperature by water flowing through the area near the output flange. The cross-section of the circular water channel can be seen in the figure.

To find an expression for the noise temperature, (7′) is expanded by dividing the cavity walls into three components: (i) the effective load surface; (ii) the wall of the cylinder, the radiation shield and the outer surfaces of the horn (including the aperture matching section just to the left of the aperture); and (iii) the internal surfaces of the horn from the aperture to the output flange:

$$T_n = T_m + \int_w (T - T_m) S' \, d\Omega + (T_h - T_m) \int_h S' \, d\Omega. \tag{17}$$

The third integral accounts for loss in the internal horn surfaces where the temperature has, for simplicity, been assumed to be constant at T_h and the

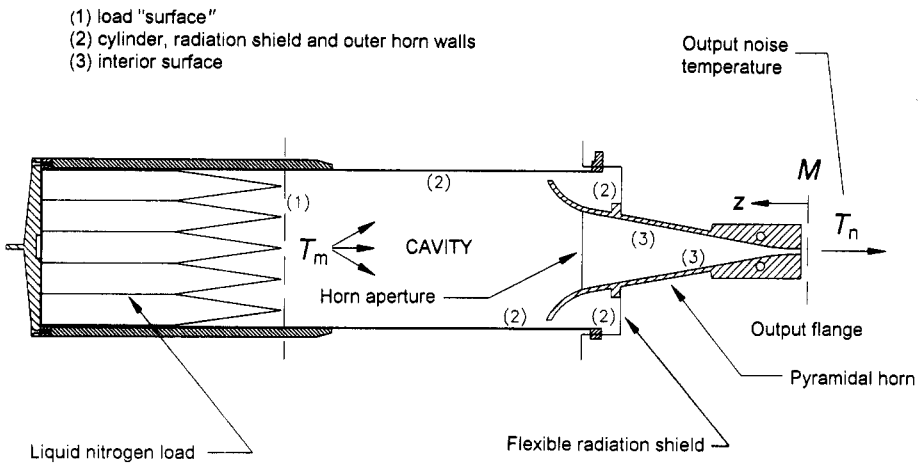

Figure 3. Horn/cavity.

difference $(T_h - T_m)$ taken out from under the integral sign.

Error calculations show that the second integral in (17) accounting for the wall losses is less than 0,05 % of the total output noise temperature. Therefore, this integral can be dropped with little error, leaving

$$T_n = T_m + (T_h - T_m) \int_h S' \, d\Omega \tag{18}$$

for the output noise temperature.

The horn is designed so that a dominant TE_{10} wave entering the output flange in Figure 3 from the right will pass through the throat and flare and radiate out from the aperture without appreciable internal reflection (measurements show this to be true to better than 0,002 in the reflection coefficient). This, along with the Lorentz reciprocity theorem [8], implies that a modal representation of the fields just to the right of the aperture consists of a dominant wave that traverses the horn to the output flange without reflection and an infinite set of evanescent waves that are completely reflected back towards the load. The load wedges (the spear-like objects in the figure), however, reflect very little of these incident evanescent waves which are almost completely absorbed. Furthermore, energy behind the horn in the region labelled (2) in the figure can only enter the aperture by diffracting around the aperture edges. This is largely prevented, however, by aperture matching the horn [9] and results in a decoupling of the aperture-flange section of the horn from the region (2) of the cavity. The implication of all this is that the section of horn from the aperture to the output flange looks like a slowly contracting waveguide to the dominant field traversing the horn from left to right, and that the integral in (18) can be replaced by (using $\alpha_2 = \alpha_h$ in (16) of the previous section)

$$\int S' \, d\Omega = 1 - \alpha_h, \tag{19}$$

where α_h is the noise efficiency of the horn. Finally, combining (18) and (19) yields

$$T_n = T_m + (T_h - T_m)(1 - \alpha_h) \tag{20}$$

for the output noise temperature of the horn/cavity.

The noise efficiency is obtained from

$$\alpha_h = 10^{-A/10}, \tag{21}$$

where A is the decibel attenuation of the horn from flange to aperture and where

$$A = \int_0^l a \, dz. \tag{22}$$

The integrand a is the power attenuation coefficient whose magnitude is a function of the distance z (see Figures 3 and 4) from the horn flange, where l is the axial flange-aperture length. This coefficient is approximated by using the standard waveguide attenuation coefficient since no such expression exists for a pyramidal horn. Coefficients for sectoral horns (Appendix B) do exist, however, and were used to estimate the error due to the waveguide approximation.

The attenuation coefficient a (normally expressed in dB/m) is plotted in Figure 4 as a function of z and helps explain one of the crucial aspects of the horn/cavity design. The excess horn noise given by the second term in (20) can be approximated by

$$(T_h - T_m)(1 - \alpha_h) \doteq 0{,}23 (T_h - T_m) A \tag{23}$$

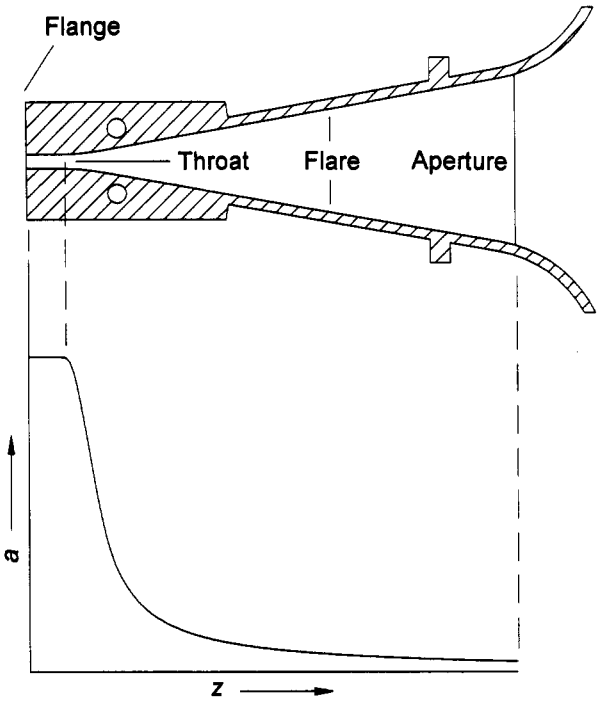

Figure 4. Attenuation coefficient.

since A is small. Thus, the excess noise is proportional to the horn attenuation: so also is the noise temperature error that results from the loss. Equation (22) shows that this attenuation is equal to the area under the attenuation coefficient curve in Figure 4. Therefore, since the flaring of the horn causes the magnitude of the coefficient to decrease rapidly away from the throat, the total attenuation, the excess noise and the error are greatly reduced over what they would be if the horn were replaced by a straight waveguide. This characteristic is important in millimetre wave noise standards where the guide loss significantly increases from band to band as the frequency increases.

5. Results and Conclusions

The most important results from the above are (7) and (7′). They are valid for any microwave cavity whatever the geometry of the cavity as long as a portion of the cavity wall has a constant temperature T_m.

The value of (7) and (7′) stems from their generality and the isolation of the dominant noise contributor T_m from the, usually, much smaller excess noise represented by the integral terms.

As pointed out above and in Appendix A, the corrections necessary to make the foregoing analysis rigorous in the quantum sense involve multiplying the thermodynamic temperatures by a simple "quantum correction" q. Performing this operation on (7′) leads to

$$T_n = q_m T_m + \int_{w+h} (q T - q_m T_m) S' \, d\Omega, \tag{24}$$

where q_m and q are given by (A.4) and (A.2) with the appropriate temperatures (T_m and T) inserted into (A.2). Expanding the parenthesis in the second term shows, however, that $q T - q_m T_m$ and $T - T_m$ differ only by a very small, second-order contribution. Thus, for practical purposes, (24) can be replaced by

$$T_n = q_m T_m + \int_{w+h} (T - T_m) S' \, d\Omega \tag{25}$$

with little error.

The horn/cavity standards designed around (25) have errors (expressed as a percentage of T_n) ranging from 0,32 % for the WR-42 band to 1,31 % for the WR-3 band [7]. In contrast, cryogenic standards built around a straight waveguide would have errors ranging from 1,58 % in WR-42 to 4,99 % in WR-3, almost a factor of 4 degradation over the horn/cavity standards.

Appendix A. Quantum Effects

The quantum effects of thermal radiation have been known since the early twentieth century [10]. Their effects are discussed here for completeness.

The brightness ($W \cdot Hz^{-1} \cdot m^{-2} \cdot sr^{-1}$) of a constant temperature surface is given by

$$B = \frac{2 hf^3}{c^2 (\exp x - 1)}, \tag{A.1}$$

where it is convenient to define

$$x \equiv \frac{hf}{kT}. \tag{A.2}$$

The quantities h, f, c, k and T are, respectively, Planck's constant, the frequency, the speed of light in a vacuum, Boltzmann's constant, and the thermodynamic temperature. It is also convenient for noise work to write (A.1) in the form

$$B = \frac{2 kq T}{\lambda^2}, \tag{A.3}$$

where

$$q \equiv \frac{x}{\exp x - 1} \tag{A.4}$$

and where λ is the wavelength corresponding to the operating frequency f.

Equation (A.3) with q equal to unity is the classical result, suggesting that the quantum counterparts to the classical results obtained earlier in the paper can be obtained by multiplying the thermodynamic temperatures in the classical equations by q, noting that the required qs are temperature-dependent because of the T in the denominator of (A.2). This is indeed true.

Appendix B. Power Attenuation Coefficients

The sectoral horn attenuation coefficients needed to evaluate the pyramidal horn mode error are not available in the open literature (although their modal fields are [11]) so they are presented in this appendix.

The attenuation coefficients can be evaluated from the modal fields and the expression [12]

$$a = 4{,}34 \frac{1}{2} \frac{1}{P} \frac{\mathrm{d}P}{\mathrm{d}z}, \tag{B.1}$$

where the "4,34" comes from 10/ln 10, P is the power travelling through the horn and $\mathrm{d}P/\mathrm{d}z$ is the corresponding loss per unit length. The propagating power and the power loss are calculated from

$$P = \frac{1}{2} \mathrm{Re} \int\int \boldsymbol{E} \times \boldsymbol{H}^* . \mathbf{dS}, \tag{B.2}$$

where $\boldsymbol{E}$ and $\boldsymbol{H}$ are the dominant mode fields, and

$$\frac{\mathrm{d}P}{\mathrm{d}z} = \frac{1}{2} R_s \int |H_\tau|^2 \, \mathrm{d}\tau. \tag{B.3}$$

The metallic surface impedance is denoted by R_s and H_τ is the dominant mode magnetic field next to the surface and parallel to the transverse dimension τ.

Rectangular waveguide

The straight waveguide result is quoted here for completeness and for comparison with the equations to follow even though the expression can be found in numerous places. The attenuation coefficient is

$$a_w = \frac{R_s}{\omega \mu \beta_g} \left(\frac{k^2}{b} + \frac{2 k_c^2}{a} \right), \tag{B.4}$$

where ω, μ, k, k_c, a and b are the radian frequency, magnetic permeability, wavenumber, cutoff wavenumber ($k_c = \pi/a$), and the broad and narrow guide dimensions. The imaginary part of the propagation constant is

$$\beta_g = k^2 - k_c^2. \tag{B.5}$$

H-plane sectoral horn

The dominant mode fields for the H-plane horn can be obtained from [11] and, after insertion into (B.1)–(B.3) (see Figure B1),

$$a_h = \frac{R_s}{\omega \mu \beta_g} \frac{1}{b} \left[k_c^2 \left(\frac{a}{2 r \theta_H} \right) \frac{|H_p^{(2)}(kr)|^2}{4 \theta_H / \pi a \beta_g} + \beta_g^2 \left(\frac{2 r \theta_H}{a} \right) \frac{|H_p^{(2)}(kr)|^2}{4 \theta_H \beta_g / \pi a k^2} + \frac{R_s}{\omega \mu \beta_g} \frac{2 k_c^2}{a} \left(\frac{a}{2 r \theta_H} \right)^2 \frac{|H_p^{(2)}(kr)|^2}{4 \theta_H / \pi a \beta_g} \right], \tag{B.6}$$

where $H_p^{(2)}$ is the Hankel function corresponding to $\exp(+\mathrm{j}\omega t)$ with fractional order p; θ_H is the half flare angle for the horn; and $H_p^{(2)'}$ is the Hankel function derivative with respect to its argument.

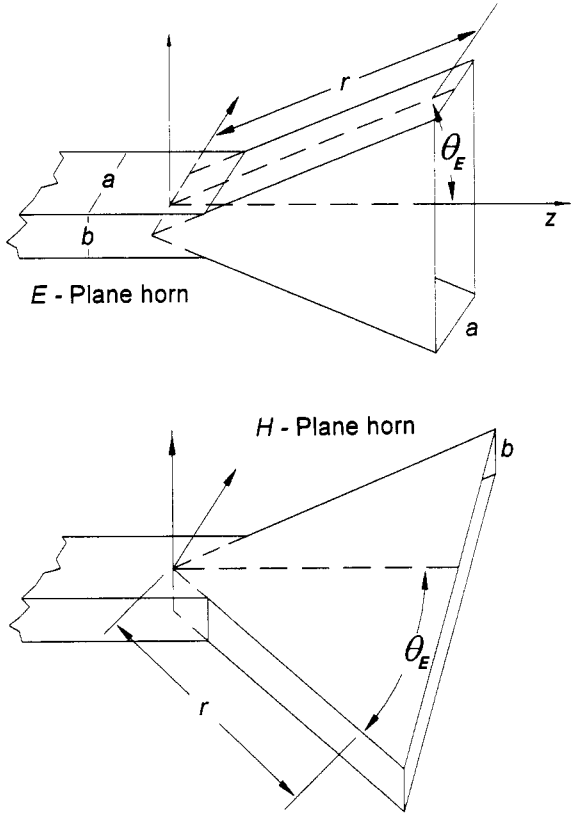

Figure B1. Sectoral horns.

***E*-plane sectoral horn**

The *E*-plane attenuation coefficient can be obtained like the *H*-plane coefficient and results in

$$a_e = \frac{R_s}{\omega\mu\beta_g}\frac{k^2}{b}\left(\frac{b}{2r\theta_E}\right)\left[\frac{|H_0^{(2)}(\beta_g r)|^2}{2/\pi\beta_g r}\right.$$

$$\left.+\left(\frac{k_c}{k}\right)^2\frac{|H_1^{(2)}(\beta_g r)|^2-|H_0^{(2)}(\beta_g r)|^2}{2/\pi\beta_g r}\right] \quad \text{(B.7)}$$

$$+\frac{R_s}{\omega\mu\beta_g}\frac{2k_c^2}{a}\frac{|H_1^{(2)}(\beta_g r)|^2}{2/\pi\beta_g r},$$

where θ_E is the half flare angle for the *E*-plane horn.

Both (B.6) and (B.7) reduce to (B.4) as θ_H and θ_E approach zero.

References

1. Daywitt W. C., *Design and Error Analysis for the WR10 Thermal Noise Standard*, Natl. Bur. Stand. (US) Tech. Note 1071, Washington, D.C., US Government Printing Office, 1983.
2. *IEEE Standard Dictionary of Electrical and Electronics Terms*, 2nd ed., IEEE Std. 100-1977, New York, Wiley-Interscience, 1977.
3. Stutzman W. L., Thiele G. A., *Antenna Theory and Design*, New York, John Wiley & Sons, 1981.
4. Miller C. K. S., Daywitt W. C., Arthur M. G., Noise Standards, Measurements, and Receiver Noise Definitions. *Proc. IEEE*, 1967, **55**, 865-877.
5. Middleton D., *An Introduction to Statistical Communication Theory*, New York, McGraw-Hill, 1960.
6. Engen G. F., *Microwave Circuit Theory and Foundations of Microwave Metrology*, London, Peter Peregrinus Ltd, 1992.
7. Daywitt W. C., A Set of Primary Noise Standards for the Millimeter Wave Bands, *Microwave Journal*, 1993, **36**, 122-126.
8. Collin R. E., *Field Theory of Guided Waves*, 2nd ed., New York, IEEE Press, 1991.
9. Burnside W. D., Chuange C. W., An Aperture Matched Horn Design, *IEEE Trans.*, 1982, **AP-30**, 790-796.
10. Joos G., Freeman I. M., *Theoretical Physics*, 3rd ed., Hafner Publishing Company, 1950.
11. *Waveguide Handbook*, Vol. 10, MIT Radiation Laboratory Series, New York, McGraw-Hill, 1951.
12. Jackson J. D., *Classical Electrodynamics*, New York, John Wiley & Sons, 1962.

Received on 11 May 1993.